Pakistan Veterinary Journal

ISSN: 0253-8318 (PRINT), 2074-7764 (ONLINE)
DOI: 10.29261/pakvetj/2026.067

RESEARCH ARTICLE

The Protective Role of YiMu-QingGong San in Lipopolysaccharide-Induced Bovine Endometrial Epithelial Cell Injury: Involving Anti-Inflammatory and Anti-Epithelial-Mesenchymal Transition

Yaming Yu[1,2], Ningning Mao[1,2], Li Liu[3], Lin Yu[1,2], Xiangwen Deng[1,2], Fangzhu Lin[1,2], Xuanqi Lu[1,2], Xiaofeng Shi[1,2], Yuyang Wei[3] and Deyun Wang[1,2,*]

[1]Institute of Traditional Chinese Veterinary Medicine, College of Veterinary Medicine, Nanjing Agricultural University, Nanjing 210095, China; [2]MOE Joint International Research Laboratory of Animal Health and Food Safety, College of Veterinary Medicine, Nanjing Agricultural University, Nanjing 210095, China; [3]Shijiazhuang Compound Veterinary Drug Industry Technology Research Institute, Shijiazhuang Shimu Pharmaceutical, Shijiazhuang, 050227, China
*Corresponding author: dywang@njau.edu.cn

ARTICLE HISTORY (25-580)

Received: June 29, 2025
Revised: February 25, 2026
Accepted: March 01, 2026
Published online: April 27, 2026

Key words:
Bovine
Endometrial epithelial cells
Endometritis
Epithelial mesenchymal transition
Inflammation

ABSTRACT

Bovine endometritis is characterized by endometrial inflammation due to bacterial infection, and the endometrial epithelium is the predominant site of bacterial infiltration. YiMu-QingGong San (YMQGS) has been validated for treating bovine endometritis, but the mechanisms regarding the regulation of endometrial epithelial cell inflammation remain unclear. This study aims to elucidate the protective effects of YMQGS against inflammatory damage in bovine endometrial epithelial cells (BEND). BEND was acted on using 10μg/mL of LPS to induce cell damage. Network pharmacology suggested that YMQGS may alleviate endometritis via the TNF, NF-κB pathway, by targeting genes such as TNF, IL-6, and IL-1β. Experimental validation demonstrated that YMQGS suppressed LPS-induced inflammation in BEND cells, with YMQGS-H displaying a potent effect by downregulating IL-6, TNF-α, and IL-1β mRNA expression by 66.67, 60.93, and 65.83%, respectively. Furthermore, YMQGS reversed LPS-induced oxidative stress and the disruption of the cellular cycle in BEND cells. We also found that LPS activated the TGF-β1 signaling pathway and promoted EMT in BEND cells, while YMQGS-H downregulated TGF-β1 protein expression by 33.93%, effectively rescuing the cells from this injury. Collectively, YMQGS mitigates LPS-induced BEND cell damage by suppressing inflammatory responses, oxidative stress, and EMT, thereby providing novel insights into its mechanisms for treating bovine endometritis.

To Cite This Article: Yu Y, Mao N, Liu L, Yu L, Deng X, Lin F, Lu X, Shi X, Wei Y and Wang D, 2026. The protective role of yimu-qinggong san in lipopolysaccharide-induced bovine endometrial epithelial cell injury: involving anti-inflammatory and anti-epithelial-mesenchymal transition. Pak Vet J, 46(4): 853-865. http://dx.doi.org/10.29261/pakvetj/2026.067

INTRODUCTION

Endometritis is a widespread and severe postpartum reproductive disorder in dairy cows, markedly compromising reproductive efficiency by provoking inflammation and structural damage in the endometrium (Carneiro *et al*., 2016). Postpartum cervical dilation, retained lochia, and placental remnants create favorable conditions for bacterial infiltration (Osawa, 2021). Among the causative agents, Gram-negative bacteria, such as *Escherichia coli*, *Trueperella pyogenes*, etc., are primary pathogens responsible for endometrial lesions (LeBlanc, 2023). Notably, *Escherichia coli*, as a keystone pathogen, adheres to cells via flagella and secretes lipopolysaccharide (LPS) to disrupt the structural integrity of cells (Zaatout, 2022). Toll-like receptor 4 (TLR4) on cell membranes recognizes LPS and activates the downstream Nuclear Factor-κB (NF-κB) pathway (Wu *et al*., 2018). This triggers an excessive release of pro-inflammatory cytokines, including interleukin-6 (IL-6), interleukin-1β (IL-1β), tumor necrosis factor-α (TNF-α), etc., and hyperactivates innate immune responses (Loyi *et al*., 2015). Substantial evidence confirms that overactivated inflammation induces overproduction of reactive oxygen species (ROS) through mitochondrial dysfunction pathways (Zhao *et al*., 2021; Zhang and Wu, 2024). Consequently, targeting these pathways represents a key strategy for preventing and managing endometritis.

Endometrial epithelial cells serve as central executors of reproductive function, maintaining microenvironmental

homeostasis for pregnancy and embryonic development through coordinated immune regulation, barrier defense, and regenerative repair mechanisms (Ruane *et al*., 2022). As bacterial invasion primarily colonizes the endometrial epithelium, direct secretion of LPS induces structural and functional damage to endometrial epithelial cells (Cui *et al*., 2020). LPS has been demonstrated to trigger persistent inflammation, oxidative damage, and fibrotic remodeling in endometrial epithelial cells (Wan *et al*., 2020; Jiang *et al*., 2024). Furthermore, LPS has been reported to provoke transforming growth factor-beta 1 (TGF-β1) autocrine production (Chen *et al*., 2024). The TGF-β1 pathway is a pivotal molecular driver of epithelial-mesenchymal transition (EMT) (Yao *et al*., 2019). Activated TGF-β1 promotes nuclear translocation of phosphorylated Smad2/3, which suppresses epithelial markers, including E-cadherin and ZO-1, and up-regulates mesenchymal proteins, including Vimentin and N-cadherin (Chen *et al*., 2017; Sun *et al*., 2019). This cascade facilitates cytoskeletal reorganization, leading to loss of endometrial epithelial cell polarity. Thus, inhibition of TGF-β1 pathway activation may attenuate endometrial epithelial cell injury.

Herbal medicine, characterized by multi-component synergy, multi-target regulation, and holistic therapeutic effects, has been widely utilized for treating endometritis (Ding *et al*., 2022; Tian *et al*., 2024). YiMu-QingGong San (YMQGS) is a patented herbal formulation integrating the traditional and modern applications of eight medicinal herbs: *Leonurus japonicus* Houtt., *Sophora flavescens* Aiton, *Cyperus rotundus* L., *Cirsium japonicum* DC., *Cirsium arvense* var. integrifolium Wimm. & Grab., *Cnidium monnieri* (L.) Cusson, *Patrinia villosa* Juss., and *Euphorbia humifusa* Willd., specifically developed for the treatment of bovine endometritis. Modern studies reveal that *Leonurus japonicus* Houtt. The key bioactive compound, leonurine, alleviates macrophage-mediated inflammatory storms by inhibiting NF-κB nuclear translocation (Dai *et al*., 2025). *Cyperus rotundus* L. has demonstrated antioxidant properties through its volatile oils (Xue *et al*., 2023). Additionally, the bioactive component of *Sophora flavescens* Aiton, matrine, blocks cascade signaling by targeting the extracellular domain of TLR4, thereby exerting anti-inflammatory effects (Mao *et al*., 2024). Given its multi-component nature, we hypothesized that YMQGS protects endometrial epithelial cells through multiple mechanisms, including anti-inflammatory and antioxidant pathways. To verify this, we employed an integrated strategy of network pharmacology and transcriptomics to predict potential pathways of YMQGS, thereby aiming to elucidate the mechanisms by which YMQGS preserves bovine endometrial epithelial cells (BEND) from LPS-induced damage.

MATERIALS AND METHODS

Experimental drug: YMQGS is an herbal formulation composed of *Leonurus japonicus* Houtt. (60g) (lot number: 240525), *Sophora flavescens* Aiton (90g) (lot number: 240401), *Cyperus rotundus* L. (50g) (lot number: 240511), *Cirsium japonicum* DC. (45g) (lot number: 220301), *Cirsium arvense* var. integrifolium Wimm. & Grab. (45g) (lot number: 220201), *Cnidium monnieri* (L.) Cusson (60g) (lot number: 230514), *Patrinia villosa* Juss. (45g) (lot number: 210101), and *Euphorbia humifusa* Willd (30g) (lot number: 210901). The raw Chinese medicine was provided by Yonggang Decoction Pieces Factory Co., Ltd. in Bozhou City, Anhui Province. The specific proportions of constituents and standardized preparation protocol were conducted in accordance with our previous experimental procedures. Briefly, the protocol involves weighing raw materials in prescribed proportions, decocting with 10 volumes deionized water for 1.5h, and collecting the initial decoction. Subsequently, add 5 volumes of deionized water for a second decoction (1h duration) and collect the filtrate. Mix the two decoctions and concentrate the mixture to 425mL, resulting in a final YMQGS concentration of 1g/mL. Then transfer the mixture to a beaker for freeze-drying treatment. In addition, in our previous study, the chemical constituents in YMQGS have been resolved by UHPLC/MS analysis (Yu *et al*., 2025).

Network pharmacology: The Traditional Chinese Medicine Systems Pharmacology Database and Analysis Platform (TCMSP) database (https://old.tcmsp-e.com/tcmsp.php) was utilized to screen and obtain the active ingredients of each component of YMQGS separately (screening criteria were OB≥30% and DL≥0.18). Corresponding gene targets were further retrieved based on the active ingredients obtained from the screening (Ru *et al*., 2014). Disease-associated targets for bovine endometritis were acquired through GeneCards (https://www.genecards.org) and DisGeNET databases (https://www.disgenet.org/). To identify common targets, we intersected the gene targets of YMQGS active ingredients with bovine endometritis-related genes. Subsequently, the intersecting target genes were uploaded to the String database (https://www.string-db.org/) to construct the target protein interactions (PPI) network map of the intersecting genes, and the analysis results of the String database were also uploaded to Cytoscape (v3.7.1) to further construct the PPI network diagram based on the degree value. Then upload the intersected target genes to the David database (https://david.ncifcrf.gov/) for GO and KEGG pathway enrichment analysis (Sherman *et al*., 2022).

Cell viability assay: BEND cells were obtained from Beina Biology (BNCC) (Batch No. 231222), with cell identification number BNCC359233. YMQGS was dissolved in DMEM medium to prepare serial dilutions (2000, 1000, 500, 250, 125, 62.5, 31.25, 15.625, and 0μg/mL). After 24h treatment with YMQGS, viability of BEND cells was assessed using the cell counting kit 8 (CCK-8) (C6005, NCM Biotech).

Experimental design: The experiment was divided into the following groups: control group (CON), LPS group (LPS), YMQGS low-dose group (YMQGS-L), YMQGS medium-dose group (YMQGS-M), and YMQGS high-dose group (YMQGS-H). Based on the cell viability assay, the concentrations of YMQGS were determined. The inflammatory response in BEND cells was induced using 10μg/mL of *Escherichia coli* (O111:B4)-derived LPS (Jiang, *et al*., 2024). After 1h of LPS pretreatment, cells were exposed to the corresponding doses of YMQGS for 24h, followed by cell collection for subsequent analyses.

To further verify TLR4/NF-κB involvement in YMQGS anti-inflammatory action, pathway inhibitor TAK-242 was applied.

Real-time PCR: Total RNA was extracted from cells in each group using the Trizol method, and reverse-transcribed into cDNA using the *PerfectStart* Uni RT&qPCR Kit (AUQ-01, Transgen). Relative gene expression was calculated using the $2^{-\Delta\Delta CT}$ method. Primer sequences are detailed in Table 1.

Table 1: Primer sequences used for RT-PCR

Primer name	Primer sequence (5′ to 3′)		Product size (bp)	GenBank accession numbers
	Forward primer	Reverse primer		
β-actin	CATCACCATCGG CAATGAGC	AGCACCGTGTTG GCGTAGAG	156	NM_1739 79.3
IL-6	ATCCTGAAGCAA AAGATCGCAG	TTGCGTTCTTTA CCCACTCGT	100	NM_1739 23.2
TNF-α	TGCTGCACTTCG GGGTAATC	GCTTGAGAAGAG GACCTGAGT	103	NM_1739 66.3
IL-1β	AACCTTCATTGC CCAGGTTTCTG	GGTCATCAGCCT CAAATAACAGC	113	NM_1740 93.1
TLR4	TGCCTTCACTAC AGGGACTT	GGGACACCACG ACAATAACC	100	NM_1741 98.6
NF-κB	ACACGTATCGAA GGACAGCC	GTCCTCCTTCAC CTCTGTGC	179	NM_0011 02101.1

Detection of cell oxidative damage indicators in BEND cells: BEND cells were treated with YMQGS for 24h, and intracellular reactive oxygen species (ROS) was detected using the ROS assay kit (CA1410, Solarbio). The DCFH-DA fluorescent probe was diluted to 10μmol/L with culture medium. Cells were incubated with the probe solution for 20min, and the results were observed under a fluorescence microscope using 488nm excitation wavelength. The mitochondrial membrane potential (ΔΨm) of BEND cells was assessed using JC-1 assay kit (C2006, Beyotime). JC-1 dye was added to the culture medium, and cells were incubated for 20minutes. The excitation wavelength of JC-1 monomer was 488nm, and the excitation wavelength of JC-1 aggregate was 525nm. The intracellular calcium ion concentration ($[Ca^{2+}]i$) was measured using $[Ca^{2+}]i$ assay kit (G1724, Servicebio). Incubate cells with Fluo-4AM detection solution for 30min and observe staining results at 488nm excitation wavelength.

Determination of BEND cell cycle: The cells were centrifuged at 1500rpm for 5min, and washed with pre-cooled PBS. Fixed in 70% ethanol (4°C, 2h), washed again, then stained with propidium iodide (PI, 10μL) and RNase A (10μL) in staining buffer (0.5mL). After 30min dark incubation (37°C), samples were analyzed by a flow cytometer.

Transcriptomics analysis: Total RNA was extracted from BEND cells in the CON, LPS, and YMQGS-H groups using the TRIzol reagent method. RNA integrity and purity were assessed, and samples with RNA integrity number (RIN)≥8.0 were subjected to reverse transcription. The qualified RNA samples were subjected to RNA sequencing at Shanghai Majorbio Bio-pharm Technology Co., Ltd., which was performed on the Illumina NovaSeq 6000 system for transcriptomic profiling. The sequencing libraries were constructed using the Illumina NovaSeq Reagent Kit. Differential expression analysis was performed with DESeq2, applying a threshold of FDR<0.05 and |log2FC|≥1 for gene screening. Data visualization and further analyses were conducted on a cloud-based platform.

Immunofluorescence staining: BEND cells were seeded on cell coverslips and treated with YMQGS. After treatment, cells were fixed with 4% paraformaldehyde at room temperature for 10min. The coverslips were then washed with PBS to remove the fixation solution. To permeabilize the cell membrane, 0.2% Triton X-100 was added and incubated at room temperature for 10min. A hydrophobic pen was used to draw circles around the coverslips. Subsequently, primary antibodies against CK18 (1:200, BSM-52058R, Bioss), TLR4 (1:200, AF7017, Affinity), p65 (1:400, 8242s, CST), TGF-β1 (1:200, BS-0103R, Bioss), ZO-1 (1:500, ab221547, Abcam), E-cadherin (1:200, 20874-1-AP, Proteintech), Vimentin (1:200, 10366-1-AP, Proteintech), and N-cadherin (1:200, 22018-1-AP, Proteintech) were added, followed by incubation overnight. Afterward, secondary antibodies labeled with FITC or Cy3 were added and incubated at room temperature for 1h in the dark. The coverslips were then stained with DAPI for nuclear counterstaining and incubated at room temperature for 10min in the dark. Finally, Results were observed under fluorescence microscope with excitation wavelengths of 488nm or 550nm.

Phalloidin Staining: BEND cells were treated with YMQGS for 24h and fixed with 4% formaldehyde for 10min. Cells were permeabilized with 0.5% Triton X-100 for 5min, then incubated with FITC-conjugated phalloidin working solution in the dark for 30min to label filamentous actin). Following triple PBS washing, nuclei were DAPI-counterstained and imaged by confocal microscopy with excitation wavelength of 488nm.

Western-blot: After 24h of YMQGS treatment, the cells were washed three times with PBS. Total protein was extracted by lysing cells with RIPA buffer and quantified using a BCA protein assay kit. Proteins were separated by SDS-PAGE and transferred to PVDF membranes. Membranes were blocked with 5% skim milk in TBST for 1h at room temperature, then incubated with primary antibodies against TGF-β1 (1:1000, 21898-1-AP, Proteintech), Smad2/3(1:1000, WL01520, Wanleibio), p-Smad2/3(1:500, WL02305, Wanleibio), and GAPDH (1:100000, 60004-1-Ig, Proteintech) overnight. Incubate the membrane with HRP conjugated secondary antibodies (1:5000, SA00001-1 and SA00001-1, Proteintech) for 1 h. Protein bands were visualized using enhanced chemiluminescence substrate and analyzed with ImageJ software to quantify band intensity.

Data analysis: Data were expressed as mean±SD and analyzed statistically using SPSS software (SPSS 27.0). Data were subjected to a one-way analysis of variance (ANOVA), and the Least Significant Difference (LSD) test was used for post hoc analysis. P<0.05 were considered significant differences.

RESULTS

Network pharmacology predicts potential targets of action for YMQGS: By retrieving active ingredients of each component of YMQGS from the TCMSP database,

we obtained the following results: 51 active ingredients from *Leonurus japonicus* Houtt., 104 from *Cyperus rotundus* L., 113 from *Sophora flavescens* Aiton, 114 from *Cnidium monnieri* (L.) Cusson, 52 from *Patrinia villosa* Juss., 38 from *Euphorbia humifusa* Willd., 42 from *Cirsium japonicum* DC., and 13 from *Cirsium arvense* var. integrifolium Wimm. & Grab. Based on the screening criteria (OB≥30%, DL≥0.18), we identified the following active ingredients: 8 from *Leonurus japonicus* Houtt., 16 from *Cyperus rotundus* L., 24 from *Sophora flavescens* Aiton, 18 from *Cnidium monnieri* (L.) Cusson, 12 from *Patrinia villosa* Juss., 7 from *Euphorbia humifusa* Willd., 7 from *Cirsium japonicum* DC., and 5 from *Cirsium arvense* var. integrifolium Wimm. & Grab. According to each active ingredient, the corresponding target proteins were retrieved, which were transformed into gene Symbol by Uniprot database, and the duplicates were removed, and a total of 270 gene targets of the active ingredients were obtained. Cytoscape was used to construct the network diagram of active ingredients and gene targets, with a total of 351 nodes and 2591 interaction lines (Fig. 1A).

The DisGeNET and GeneCards databases were searched for the gene targets of endometritis in dairy cows, and 210 gene targets of endometritis in bovine were obtained by removing duplicates. Through cross-referencing YMQGS active component targets with these disease targets, we obtained 26 overlapping genes. PPI network was constructed by the String database, revealing 26 nodes and 211 interaction edges with an average node degree of 16.2. The PPI data were visualized using Cytoscape, followed by further construction of a drug-disease target interaction network (Fig. 1B and C). According to the above results, TNF, IL-6, and IL-1β may be the main core targets of action of this YMQGS for the treatment of endometritis in cows.

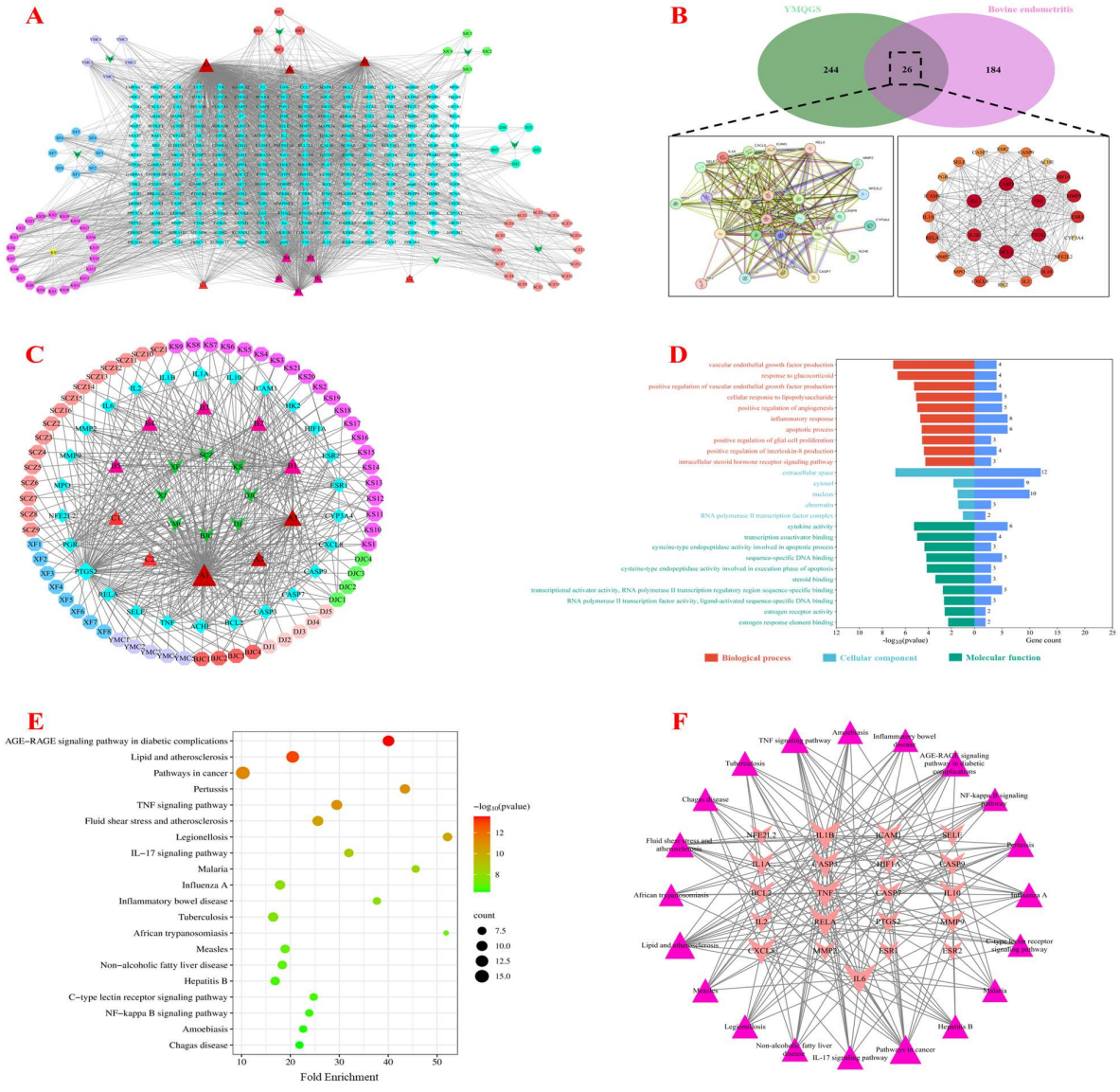

Fig. 1: Network pharmacology prediction of potential therapeutic targets for YMQGS in the prevention and treatment of bovine endometritis. (A) Network diagram of YMQGS active ingredients and targets of action. (B) Venn diagram of YMQGS and bovine endometritis-related gene targets, with a PPI network of overlapping genes. (C) Target network of YMQGS active ingredients and overlapping genes. (D) GO functional enrichment analysis of overlapping genes. (E) KEGG pathway enrichment analysis of overlapping genes. (F) Network visualization of KEGG-enriched pathways and their associated overlapping genes.

Gene Ontology (GO) functional enrichment analysis of the overlapping genes revealed 114 biological process (BP) items, 5 cellular component (CC) items, and 24 molecular function (MF) items. The top 10 BP and MF terms, along with all CC terms, were selected for visualization (Fig. 1D). BP terms primarily included cellular response to lipopolysaccharide, inflammatory response, etc., CC terms involved extracellular space, cytoplasm, nucleus, etc., and MF terms featured cytokine activity. KEGG pathway enrichment analysis identified 85 enriched pathways ($P<0.05$), with the top 20 significantly enriched pathways visualized in a bubble plot (Fig. 1E). The relevant pathways involved mainly included several signaling pathways that regulate inflammatory responses, such as TNF signaling pathway, NF-κB signaling pathway, etc., which might be the main regulatory pathways in the treatment of bovine endometritis with YMQGS (Fig. 1F).

YMQGS reduces LPS-induced expression of inflammatory factors in BEND cells: As Fig. 2A demonstrated the identification of BEND cells, the morphology of BEND cells was irregularly polygonal under light microscopy. Furthermore, CK18, a marker for endometrial epithelial cells, was observed to be highly expressed by BEND cells. Fig. 2B displayed the CCK-8 assay results for cell viability. YMQGS significantly inhibited BEND cell viability at a concentration of 2000μg/mL ($P<0.01$). Therefore, subsequent experiments were conducted at 1000, 500 and 250μg/mL. LPS treatment upregulated mRNA expression of IL-6, TNF-α, and IL-1β in BEND cells, confirming LPS-induced inflammatory responses. YMQGS downregulated these pro-inflammatory cytokines, with YMQGS-H showing pronounced inhibitory effects ($P<0.01$; Fig. 2C-E). Compared with the LPS group, the YMQGS-H group downregulated IL-6, TNF-α, and IL-1β mRNA expression by 66.67, 60.93, and 65.83%, respectively. These results preliminarily validate the ability of YMQGS to suppress LPS-triggered inflammatory responses in BEND cells.

YMQGS inhibits LPS-induced activation of the TLR4/NF-κB pathway: TLR4, the primary receptor for LPS, mediates LPS-induced innate immune responses, with the NF-κB pathway being one of its key downstream inflammatory cascades. Our results demonstrated that compared to the CON group, the LPS group exhibited elevated mRNA expression of TLR4 and NF-κB ($P<0.01$). All YMQGS groups reduced TLR4 and NF-κB mRNA levels, effectively inhibiting TLR4/NF-κB pathway activation ($P<0.01$; Fig. 2F and G). Immunofluorescence staining further corroborated these findings, showing YMQGS suppressed TLR4 protein expression and nuclear translocation of p65, confirming its inhibitory effect on TLR4/NF-κB pathway (Fig. 2H-K). To further validate YMQGS-mediated inhibition of the TLR4/NF-κB pathway, we employed TAK-242 to block TLR4 activation. Immunofluorescence staining revealed that TAK-242 group did not significantly affect TLR4 protein expression compared to LPS group, while markedly inhibited p65 nuclear translocation ($P<0.01$), indicating its selective suppression of TLR4 downstream signaling. Conversely, YMQGS and YMQGS+TAK-242 groups downregulated TLR4 protein expression and suppressed p65 nuclear translocation compared to LPS group. Importantly, YMQGS+TAK-242 demonstrated greater inhibition of TLR4 protein levels and p65 nuclear translocation than TAK-242 alone ($P<0.01$), suggesting synergistic inhibition of NF-κB activation by YMQGS and TAK-242 (Fig. 3A-D). The above results collectively demonstrated that YMQGS inhibited LPS-induced activation of the TLR4/NF-κB pathway in BEND cells.

YMQGS attenuates LPS-induced oxidative damage and regulates cell cycle in BEND cells: LPS has been demonstrated to induce intracellular oxidative stress responses (Mao *et al*., 2024). We therefore evaluated whether YMQGS could protect BEND cells from damage by mitigating oxidative stress. DCFH-DA, an optimal fluorescent probe for detecting intracellular ROS, was employed. As shown in Fig. 4A, green fluorescence (representing DCFH-DA signals) revealed significantly higher relative intensity in LPS-treated BEND cells compared to the CON group. YMQGS dose-dependently reduced ROS production, with all treatment groups showing statistically significant reductions ($P<0.01$) (Fig. 4A and D). Excessive ROS can attack mitochondrial membranes, induce lipid peroxidation, and impair mitochondrial function. Subsequently, we assessed ΔΨm using the JC-1 fluorescent probe, where the JC-1 aggregates/monomers ratio serves as an indicator of ΔΨm dynamics. In the CON group, JC-1 predominantly existed as aggregates. Compared to CON group, LPS-treated BEND cells showed increased JC-1 monomers and a significantly reduced aggregates/monomers ratio ($P<0.01$), indicating ΔΨm depolarization. The YMQGS dose groups significantly reduced the production of JC-1 monomer to inhibit the decrease in the JC-1 aggregates/monomer ratio due to LPS and to reduce the damage to the mitochondrial membrane ($P<0.05$ or $P<0.01$) (Fig. 4B and E). ΔΨm, as an electrochemical gradient between the inner and outer mitochondrial membranes, is an important factor in the regulation of cellular $[Ca^{2+}]i$ homeostasis. Normal ΔΨm drives Ca^{2+} into mitochondria, and when ΔΨm is reduced, mitochondrial calcium uniporter activity decreases, leading to reduced mitochondrial uptake of Ca^{2+} and elevated $[Ca^{2+}]i$ levels, which in turn triggers cell injury. In our assay of $[Ca^{2+}]i$, we found that LPS significantly elevated cellular $[Ca^{2+}]i$ content, whereas $[Ca^{2+}]i$ content was reduced in YMQGS-M and YMQGS-H groups ($P< 0.01$) (Fig. 4C and F). Based on these results, it was indicated that YMQGS inhibited ROS generation and decreased mitochondrial membrane potential, reduced cellular $[Ca^{2+}]i$ accumulation, and protected BEND cells from oxidative damage. Under the dual stressors of inflammation and oxidative damage, sustained cellular injury may occur. Flow cytometric analysis of BEND cell cycle progression revealed that compared to the CON group, LPS treatment significantly decreased the S-phase population while increasing G0/G1 and G2/M phase proportions ($P<0.01$). All YMQGS dose groups counteracted LPS-induced S-phase reduction and G0/G1-phase elevation. Notably, the YMQGS-H group significantly reduced the G2/M-phase population compared to the LPS group ($P<0.05$ or $P<0.01$) (Fig. 4G and H). The above results suggested that YMQGS could reverse the LPS-induced reduction of S phase and elevation of G0/G1 phase, and alleviate LPS-induced cell cycle block, in which the YMQGS-H group reduced the ratio of G2/M phase, which might be involved in the process of DNA repair.

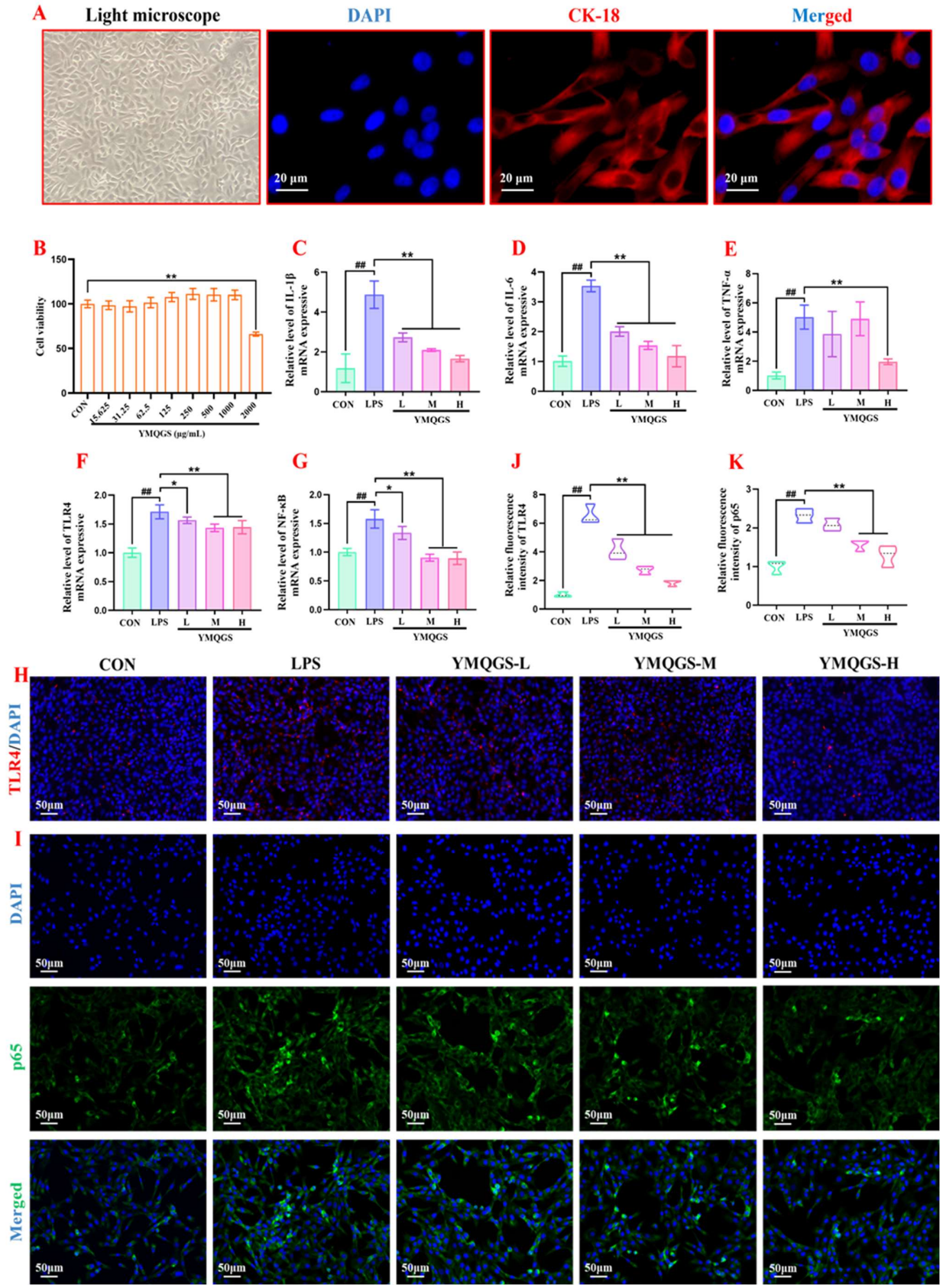

Fig. 2: YMQGS alleviates inflammatory responses in BEND cells. (A) Morphology of BEND cells under light microscope and immunofluorescence staining with CK18. (B) Changes in BEND cell viability (n=5). (C), (D), (E), (F), (G) mRNA expression of IL-1β, IL-6, TNF-α, TLR4, and NF-κB in BEND cells (n=4). (H), (I) Immunofluorescence staining of TLR4 and p65. (J), (K) Quantification of TLR4 and p65 immunofluorescence intensity (n=3). Data are shown as mean±SD, $^{\#\#}P<0.01$ vs. the CON group, $^{*}P<0.05$, $^{**}P<0.01$ vs. the LPS group.

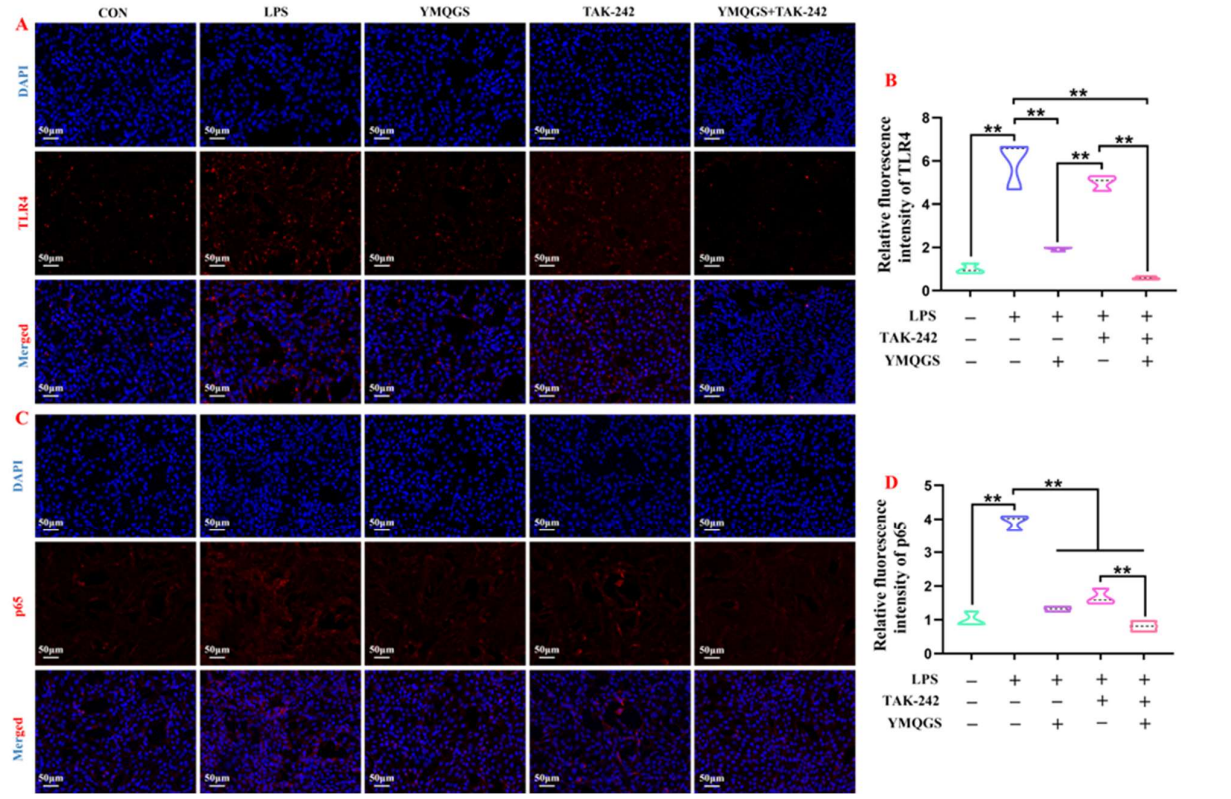

Fig. 3: TAK-242 validates YMQGS-mediated inhibition of TLR4/NF-κB signaling pathway activation. (A), (C) Immunofluorescence staining of TLR4 and p65 in BEND cells after TAK-242 treatment (n=3). (B), (D) Quantification of TLR4 and p65 immunofluorescence intensity after TAK-242 treatment (n=3). Data are shown as mean±SD, *P<0.05, **P<0.01, comparison between two groups.

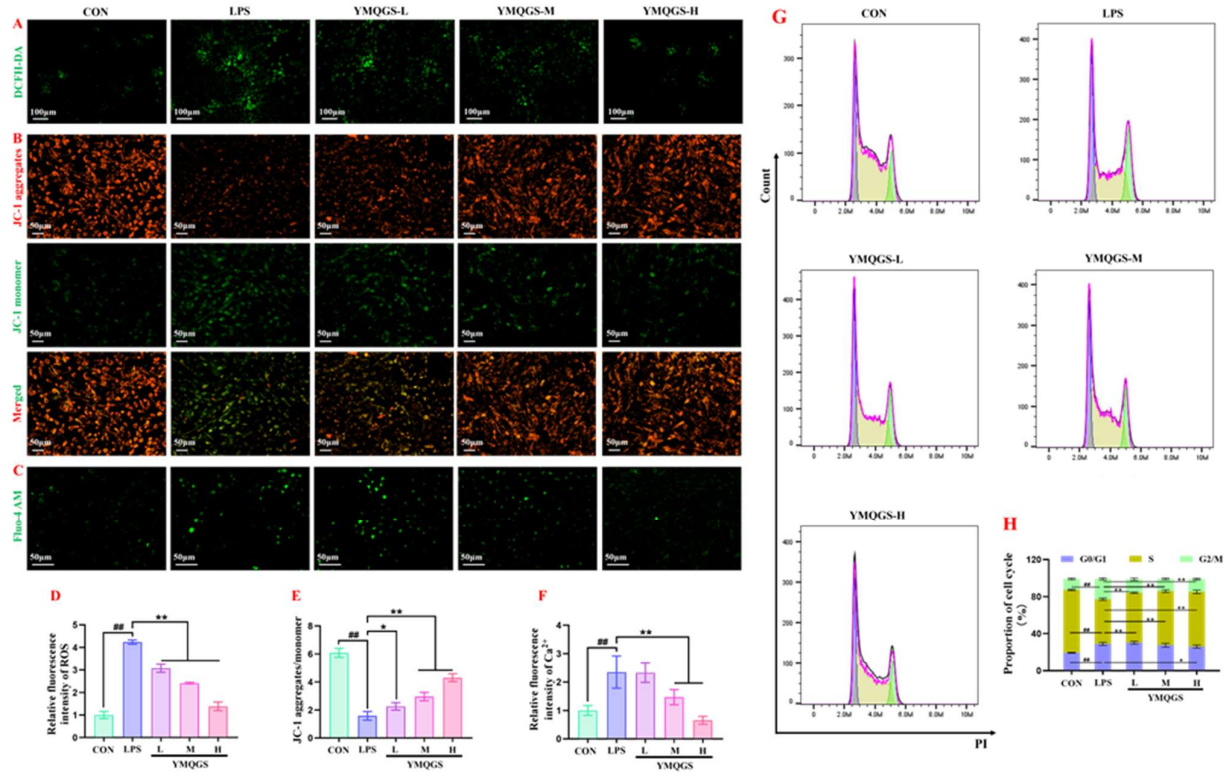

Fig. 4: YMQGS alleviates oxidative damage and modulates cell cycle progression in BEND cells. (A) DCFH-DA fluorescent probe. (B) JC-1 fluorescent probe. (C) Fluo-4 AM fluorescent probe. (D) Quantification of relative intracellular ROS levels (n=3). (E) Ratio of JC-1 aggregates to monomers (n=3). (F) Quantification of relative intracellular $[Ca^{2+}]i$ levels (n=3). (G) Flow cytometric analysis of BEND cell cycle distribution. (H) Quantification of cell cycle phase distribution (n=4). Data are shown as mean±SD, $^{\#\#}$P<0.01 vs. the CON group, *P<0.05, **P<0.01 vs. the LPS group.

Transcriptomics analysis: Building on the aforementioned studies demonstrating the multifaceted protective effects of YMQGS (L/M/H) against LPS-induced BEND cell damage in a dose-dependent manner, with YMQGS-H exhibiting optimal efficacy. In order to further analyze the molecular protective mechanism of YMQGS-H, transcriptomics was used to explore the characteristics of differentially expressed gene profiles, the dynamics of key signaling pathways and the potential regulatory network interactions. Fig. 5A shows the correlation analysis between the groups of samples, demonstrating that there is a strong correlation between the groups of biological replicates, which can be used for further subsequent analyses. Principal component analysis (PCA) revealed distinct gene expression profiles between the LPS group and both the CON and YMQGS groups (Fig. 5B). The cumulative proportion of variation for PC1, PC2, and PC3 is 52.88%, representing approximately 52.88% of the biological and technical variations in the dataset. PC1 alone explains 30.37% of the total variance, serving as the most significant separating factor among the three components and reflecting core biological differences. PC2 and PC3 account for 12.25 and 10.26% of the variance, respectively, which may be associated with other biological responses. Differential expression genes (DEGs) analysis using DESeq2 revealed 427 upregulated and 550 downregulated genes in the LPS group compared to the CON group, while YMQGS treatment resulted in 1374 upregulated and 1148 downregulated genes relative to the LPS group (Fig. 5C and D). Hierarchical clustering heatmaps of DEGs between CON vs. LPS and LPS vs. YMQGS are shown in Fig. 5E and F, respectively. GO enrichment analysis demonstrated that LPS-treated cells were predominantly enriched in processes such as regulation of cellular process, nucleus, intracellular organelle, cytoplasm, binding, protein binding, etc. (Fig. 5G). YMQGS-treated cells exhibited similar GO enrichment profiles (biological processes, cellular components, molecular functions) relative to the LPS group (Fig. 5H). KEGG pathway analysis identified significant enrichment in Adherens junction, Bacterial invasion of epithelial cells, and TGF-β signaling pathways in the LPS group versus CON (Fig. 5I). Notably, YMQGS treatment similarly enriched pathways including Tight junction, Bacterial invasion of epithelial cells, Adherens junction, and TGF-β signaling compared to LPS (Fig. 5J). These enrichment patterns collectively suggest that YMQGS protects BEND cells by synergistically inhibiting pathogen invasion-associated signaling, modulating TGF-β pathways, and restoring epithelial barrier integrity. Integrated transcriptomic profiling indicates that YMQGS may reverse LPS-induced BEND cell damage through a multi-target mechanism involving coordinated regulation of inflammatory responses, epithelial barrier function, and TGF-β-mediated repair processes.

YMQGS inhibits LPS-induced activation of the TGF-β1 pathway: According to transcriptomic screening results, we further validated the role of the TGF-β signaling pathway. Compared to the CON group, LPS-treated BEND cells exhibited significantly elevated protein expression of TGF-β1 and Smad2/3 ($P<0.05$ or $P<0.01$). Conversely, YMQGS downregulated TGF-β1 and Smad2/3 protein levels compared to the LPS group, with YMQGS-H showing the most significant effect, downregulating TGF-β1 by 33.93% ($P<0.05$ or $P<0.01$) (Fig. 6A-C). Immunofluorescence staining further revealed YMQGS-mediated suppression of LPS-induced TGF-β1 overexpression (Fig. 6D and E). These findings collectively confirmed that YMQGS inhibited activation of the TGF-β1/Smad2/3 signaling axis.

YMQGS blocks the transformation of BEND cell polarity: The BEND cells exhibit inherent polarity under physiological conditions; however, inflammatory stimuli may induce epithelial-mesenchymal transition (EMT) in BEND cells, compromising epithelial barrier integrity. Studies demonstrate that TGF-β1 regulates EMT progression (Yao *et al*., 2019; Deng *et al*., 2022). ZO-1 acts as a tight junction protein between epithelial cells and maintains the barrier function of epithelial cells, whereas when EMT occurs, the epithelial cells will lose their polarity and acquire mesenchymal cell properties. The results showed that ZO-1 expression was significantly reduced in the LPS group compared with the CON group, while YMQGS could upregulate ZO-1 expression (Fig. 7B). Phalloidin staining revealed cytoskeletal changes in BEND cells. Compared to the CON group, which exhibited a polygonal morphology characteristic of epithelial cells, LPS treatment induced an elongated spindle-shaped cytoskeletal structure in BEND cells, indicative of mesenchymal cell traits. Notably, YMQGS reversed these LPS-induced cytoskeletal alterations (Fig. 7A). E-cadherin, an epithelial cell marker, was downregulated following LPS treatment, while mesenchymal markers Vimentin and N-cadherin were upregulated, further evidencing LPS-induced EMT progression in BEND cells. YMQGS mitigated LPS-mediated E-cadherin suppression and attenuated the upregulation of Vimentin and N-cadherin, demonstrating its inhibitory effect on BEND cell polarity transition (Fig. 7C). These findings indicated that YMQGS inhibited BEND cell polarity transition and mitigates EMT progression.

DISCUSSION

Postpartum endometritis is a highly prevalent reproductive disorder in dairy cows during the peripartum period, clinically characterized by persistent endometrial inflammation (Carneiro *et al*., 2016). This condition leads to abrupt declines in milk production, significant reproductive impairment, and increased involuntary culling rates, posing dual threats to bovine health and the dairy industry. Global economic losses attributable to these impacts are estimated to exceed billions of dollars annually (Amin *et al*., 2023). However, current antibiotic-centric therapeutic strategies face diminishing clinical efficacy compelling researchers to explore novel multi-target synergistic interventions (Haimerl and Heuwieser, 2014). YMQGS, as an herbal formula for the treatment of bovine endometritis, has demonstrated clinical efficacy, though its mechanistic underpinnings remain incompletely understood. In the present study, the multi pathway synergistic mechanism of YMQGS in protecting BEND cells was revealed as shown in Fig. 8. Unlike traditional single target drugs, YMQGS not only alleviates

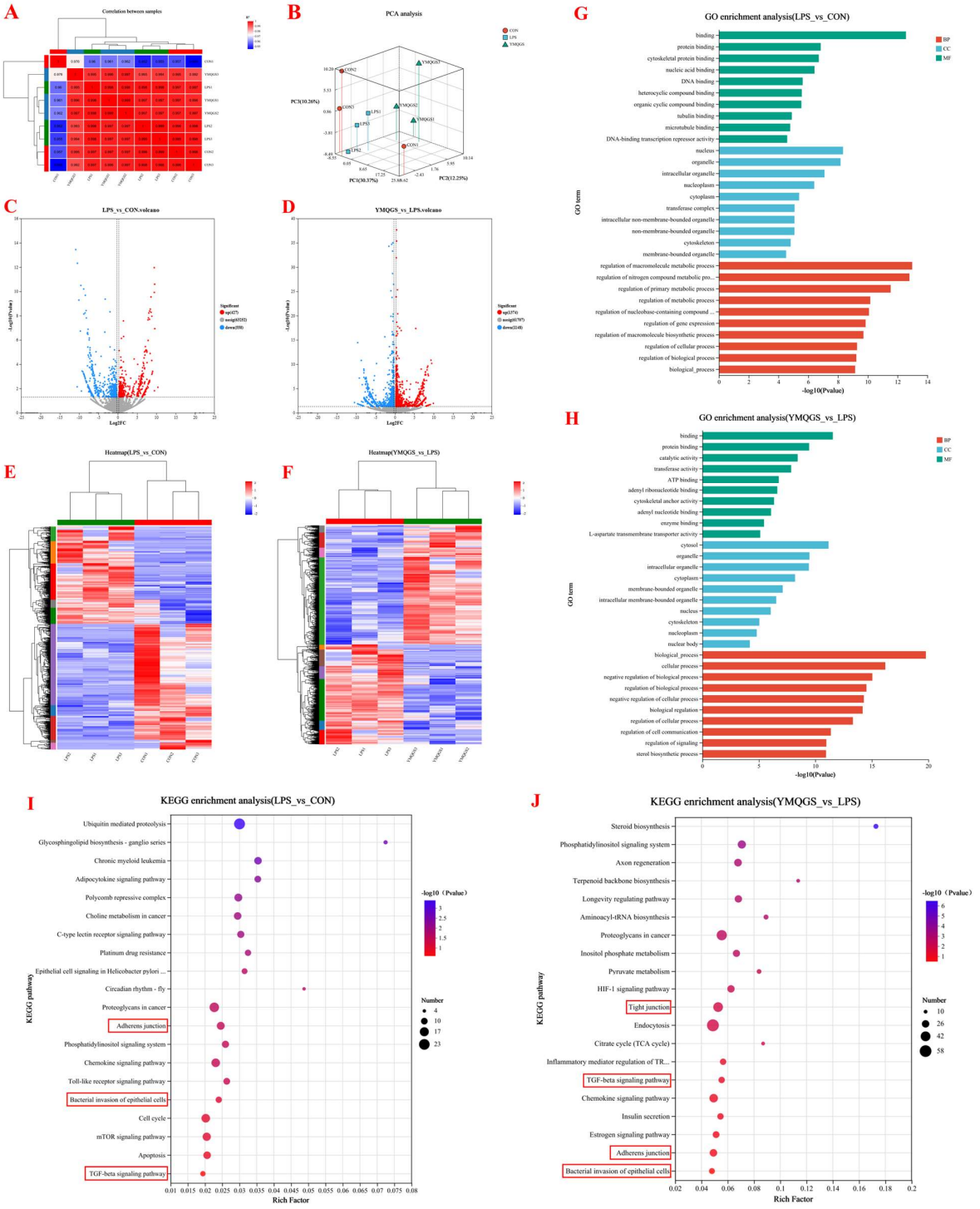

Fig. 5: Transcriptomic profiling of BEND cells (n=3). (A) Correlation analysis between samples. (B) PCA analysis of gene expression profiles. (C), (D) Volcano plot of DEGs. (E), (F) Heatmap of DEG clustering. (G), (H) GO functional enrichment analysis. (I), (J) KEGG pathway enrichment analysis.

inflammation and oxidative damage through the known TLR4/NF-κB and ROS inhibition pathways, but more importantly, a new mechanism has been discovered by mediating TGF-β1 pathway to inhibit EMT and repair epithelial barrier function. This multi-target mode of action underscores the potential of YMQGS as traditional Chinese medicine formulation in treating endometritis with comprehensive therapeutic advantages.

Network pharmacology analysis integrates bioinformatics, chemical component profiling, and pharmacodynamic evaluation to identify potential therapeutic targets by correlating active ingredients of herbs with disease-related genes (Ru *et al*., 2014; Li *et al*., 2022). In this study, we constructed the target interaction network between YMQGS and bovine endometritis, identifying 29 overlapping gene targets. Key overlapping

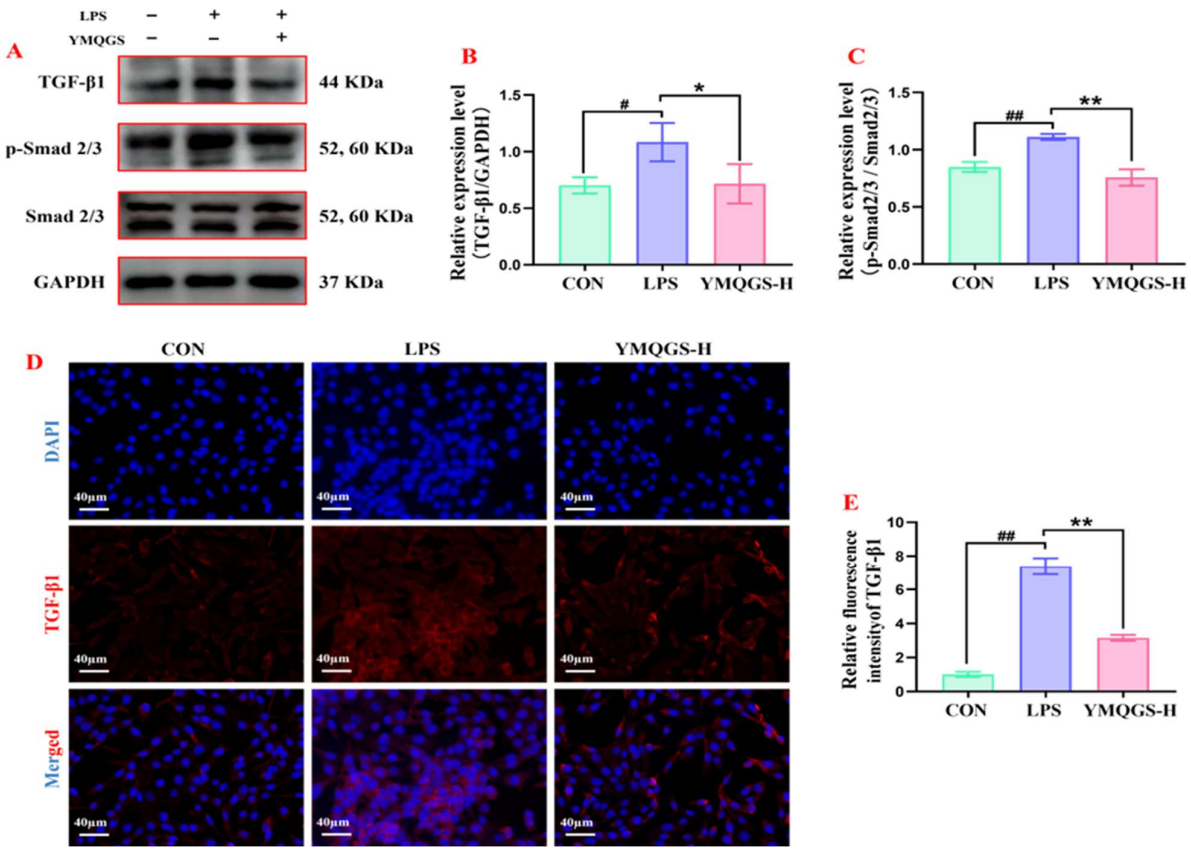

Fig. 6: YMQGS inhibits activation of the TGF-β1/Smad2/3 signaling pathway. (A) Western blotting visualization of TGF-β1 and Smad2/3 protein expression. (B) Relative protein expression levels of TGF-β1 normalized to GAPDH (n=3). (C) Relative protein expression levels of p-Smad2/3 total Smad2/3 (n=3). (D) Immunofluorescence staining of TGF-β1. (E) Quantification of TGF-β1 immunofluorescence intensity (n=3). Data are shown as mean±SD, $^{\#}P<0.05$, $^{\#\#}P<0.01$ vs. the CON group, $^{*}P<0.05$, $^{**}P<0.01$ vs. the LPS group.

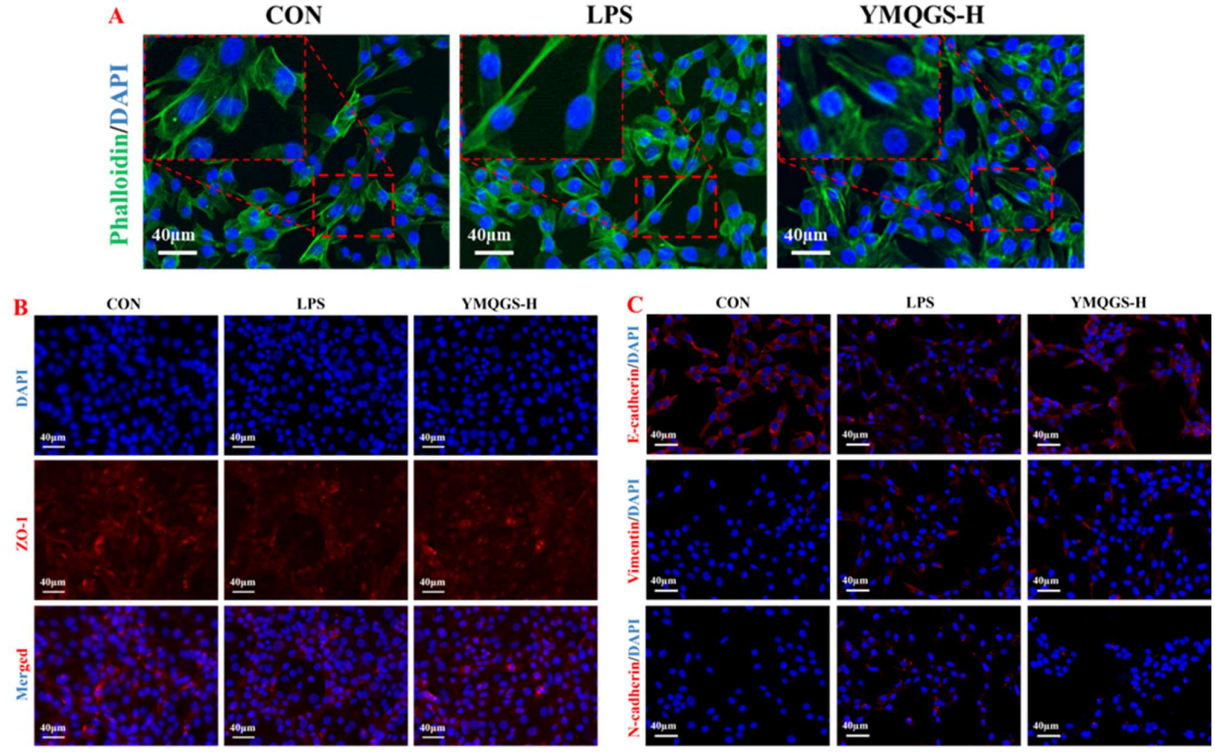

Fig. 7: YMQGS inhibits polarity transition in BEND cells (n=3). (A) Phalloidin staining of cytoskeletal morphology. (B) Immunofluorescence staining of ZO-1. (C) Immunofluorescence staining of E-cadherin, Vimentin, and N-cadherin in BEND cells.

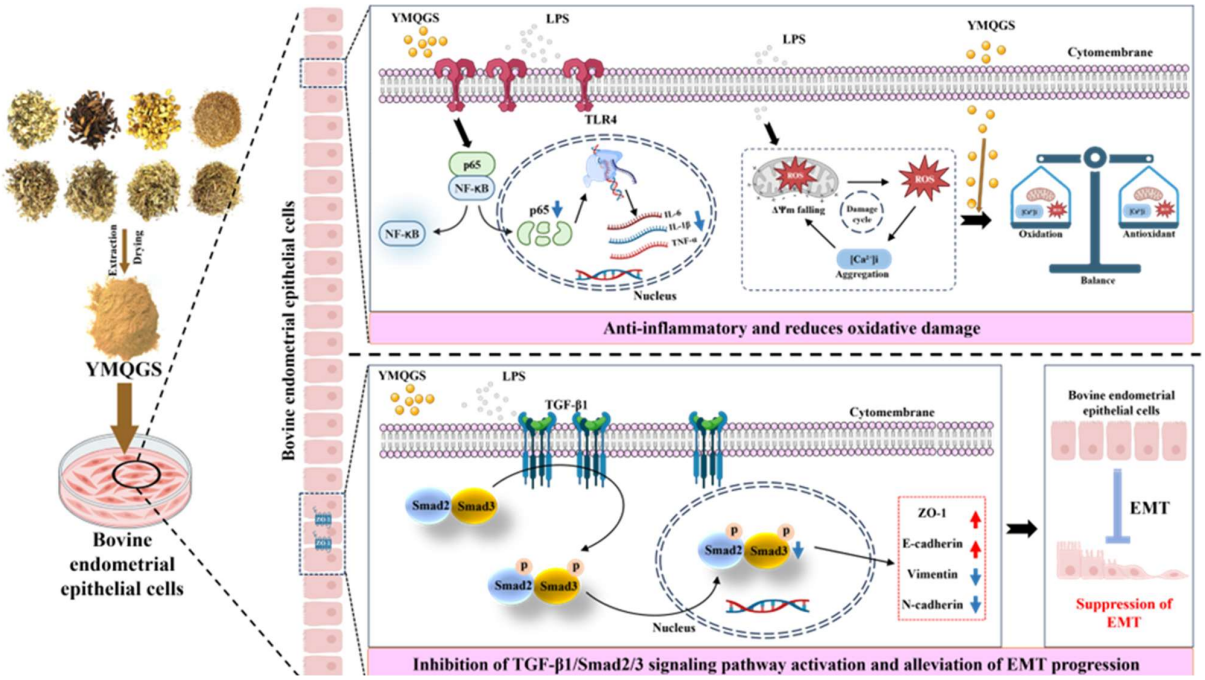

Fig. 8: Schematic diagram of YMQGS-mediated protective mechanisms against LPS-induced damage in BEND cells. YMQGS could inhibit the TLR4/NF-κB pathway to alleviate LPS-triggered inflammatory responses; modulate oxidative-antioxidant homeostasis to mitigate oxidative damage; and suppress LPS-induced EMT in BEND cells. TLR4/NF-κB pathway is a classical inflammatory response pathway. LPS binds to the TLR4 receptor on the cell membrane, activating downstream NF-κB signaling and promoting its translocation into the nucleus, where it initiates the expression of numerous pro-inflammatory cytokines. LPS can also induce oxidative stress, involving the release of ROS, decrease in ΔΨm, and accumulation of intracellular Ca^{2+}. Additionally, TGF-β1 can phosphorylate and activate Smad2/3 proteins, mediating the EMT process.

targets, including TNF, IL-6, and IL-1β, exhibited high relevance to both YMQGS and endometritis pathogenesis. Research indicates that bovine endometritis arises from uterine microbial dysbiosis, characterized by increased relative abundance of pathogens linked to luminal epithelial damage, which triggers inflammatory cell infiltration and production of cytokines such as TNF-α and IL-6, consistent with our identified targets (Bogado Pascottini *et al*., 2023). GO and KEGG enrichment analyses of overlapping genes revealed predominant enrichment in inflammation-regulating pathways, notably the TNF and NF-κB signaling cascades, suggesting that YMQGS may alleviate endometritis primarily through anti-inflammatory mechanisms.

During the postpartum period in dairy cows, the uterus is highly susceptible to Gram-negative bacterial infections due to parturition-induced tissue damage and immunosuppression (Owens *et al*., 2020). LPS, as a key virulence factor of Gram-negative bacteria, has been widely adopted as an ideal experimental tool to mimic inflammatory cascades in endometritis research due to its robust activation of TLR4, mirroring natural infection contexts (Zhang *et al*., 2019; Shaukat *et al*., 2025). This study simulated the imbalance of epithelial immune response, providing a controllable experimental model for understanding the molecular mechanism and drug intervention of endometritis. Results demonstrated that LPS elevated TLR4 and NF-κB expression, promoted p65 nuclear translocation, and induced transcription of IL-6, TNF-α, and IL-1β, confirming LPS-induced inflammatory activation in BEND cells. YMQGS treatment suppressed LPS-triggered TLR4/NF-κB pathway activation and reduced pro-inflammatory cytokine production. TAK-242 acts as a small molecule inhibitor that directly binds to the intracellular TIR structural domain of TLR4 and blocks downstream signal transduction (Matsunaga *et al*., 2011). Validation using TAK-242 revealed that TAK-242 did not affect TLR4 and inhibited the expression of NF-κB, and YMQGS exhibited similar inhibition of NF-κB activation. This confirmed that YMQGS could attenuate the inflammatory response of BEND cells by inhibiting TLR4/NF-κB pathway activation, which corroborated with the results of the network pharmacological predictions.

Existing studies have demonstrated that in inflammatory responses, cytokines such as TNF-α and IL-1β activate NADPH oxidase and disrupt mitochondrial electron transport chains, leading to explosive accumulation of ROS (Song *et al*., 2022; Shaukat *et al*., 2024). Excess ROS can directly oxidize mitochondrial membrane lipids and reduces ΔΨm, exacerbating the inflammatory microenvironment (Sinha *et al*., 2013; Moustakli *et al*., 2025). The decline in ΔΨm impairs mitochondrial calcium buffering capacity, while cytosolic Ca^{2+} overload further activates calcium-dependent proteases and endoplasmic reticulum stress, driving inflammation-associated oxidative stress (Tang *et al*., 2013; Korotkov, 2023). Our current study revealed that LPS triggers a cascade of oxidative stress, mitochondrial dysfunction, and calcium overload in BEND cells through inflammatory activation, while YMQGS interrupts this vicious cycle via multi-target interventions. Additionally, LPS induced cell cycle arrest in BEND cells, which was reversed by YMQGS. Notably, YMQGS (1000μg/mL) reduced the G2/M phase proportion, suggesting its potential to promote cell cycle progression by repairing DNA double-strand breaks or regulating Wee1 kinase

(Zhang *et al*., 2024). The inhibition of oxidative stress and regulation of cell cycle progression underscore a unique cytoprotective mechanism of YMQGS, which may achieve cellular protection through pro-repair strategies rather than solely relying on anti-oxidative interventions.

EMT refers to a dynamic process wherein epithelial cells lose polarity and intercellular junction properties through phenotypic reprogramming, while acquiring mesenchymal migratory and invasive capabilities (Lamouille *et al*., 2014). Aberrant EMT activation is closely associated with pathological conditions such as endometriosis, impaired endometrial receptivity, and fibrotic remodeling. TGF-β1, a core driver of this process, accelerates fibrogenesis and EMT progression via the Smad2/3-dependent signaling axis (Balasubramanian *et al*., 2021; Katsuno and Derynck, 2021). In the present study, transcriptomic analysis revealed that LPS-induced BEND cell injury was enriched in biological processes including inflammatory response, TGF-β signaling pathway, tight junction, etc., suggesting that EMT may mediate the LPS-induced BEND cell injury cascade. Further experiments showed that LPS stimulation up-regulated the expression of TGF-β1 and its downstream phosphorylated Smad2/3 proteins, which may be related to the enhancement of TGF-β autocrine feedback induced by the activation of TLR4/NF-κB pathway. Phenotypic analysis confirmed that LPS treatment induced characteristic EMT transition in BEND cells, manifested by downregulation of epithelial markers ZO-1 and E-cadherin, upregulation of mesenchymal markers Vimentin and N-cadherin, cytoskeletal reorganization, which is consistent with previous study (Sun *et al*., 2024). Importantly, YMQGS intervention not only impeded EMT progression by inhibiting TGF-β1/Smad2/3 pathway but also specifically upregulated tight junction protein ZO-1 expression and preserved epithelial cytoskeletal architecture. YMQGS restored cellular polarity through the dual mechanism of molecular signaling inhibition and physical barrier remodeling, which provided a novel intervention strategy for targeting the EMT-associated endometrial pathologies.

In the present study, YMQGS protects BEND cells from LPS-induced damage by modulating the TLR4/NF-κB and TGF-β1/Smad2/Smad3 pathways. However, whether there is crosstalk between these two pathways in mediating this protective effect remains unclear, presenting a direction for future research. Furthermore, building on these *in vitro* findings, we plan to establish an LPS-induced endometritis model *in vivo* to investigate whether YMQGS and its active ingredients alleviate endometrial barrier damage by suppressing EMT. This study will systematically explore its synergistic mechanisms in modulating the inflammatory microenvironment, inhibiting fibrosis, and promoting tissue repair, thereby providing further mechanistic evidence for the clinical application of YMQGS in treating bovine endometritis.

Conclusions: This study systematically revealed the multi-pathway protective mechanism of YMQGS against inflammatory pathological processes in endometrial epithelial cells by constructing an LPS-induced BEND cell injury model. YMQGS could suppress pro-inflammatory cytokine expression by inhibiting activation of TLR4/NF-κB pathway, confirming its anti-inflammatory efficacy through targeted regulation of canonical inflammatory pathways. YMQGS dose-dependently scavenged excessive ROS, stabilized $\Delta\Psi m$, and alleviated Ca^{2+} overload, thereby blocking oxidative stress cascades via restoration of redox balance and preservation of organelle functionality. Additionally, we identified that LPS induces EMT in BEND cells, while YMQGS reversed EMT-related marker dysregulation and inhibited cytoskeletal remodeling, effectively maintaining epithelial barrier integrity. Collectively, YMQGS protects BEND cells from LPS-induced damage through multi-mechanism synergy, providing experimental evidence for developing natural product-based, multi-target therapeutic strategies against endometritis.

Declaration of Competing Interest: The authors declare that they have no competing interests.

Authors Contribution: YY: Writing–original draft, Validation, Methodology, Data curation, Conceptualization; NM: Validation, Methodology, Data curation; LL: Investigation, Methodology; LY: Methodology, Investigation; XD: Validation, Methodology; FL: Validation, Methodology; XL: Validation, Visualization; XS: Visualization; YW: Methodology; DW: Supervision, Project administration, Funding acquisition.

Acknowledgements: This work is funded by the National Key Research and Development Program (Grant No. 2022YFD1801103), the Fundamental Research: Funds· for the Central Universities (Grant No. KYCXJC2025002).

REFERENCES

Amin YA, Abdelaziz SG and Said AH, 2023. Treatment of postpartum endometritis induced by multidrug-resistant bacterial infection in dairy cattle by green synthesized zinc oxide nanoparticles and in vivo evaluation of its broad spectrum antimicrobial activity in cow uteri. Research in Veterinary Science 165:105074.

Balasubramanian V, Saravanan R, Joseph LD, *et al*., 2021. Molecular dysregulations underlying the pathogenesis of endometriosis. Cell Signalling 88:110139.

Bogado Pascottini O, LeBlanc SJ, Gnemi G, *et al*., 2023. Genesis of clinical and subclinical endometritis in dairy cows. Reproduction 166:R15-R24.

Carneiro LC, Cronin JG and Sheldon IM, 2016. Mechanisms linking bacterial infections of the bovine endometrium to disease and infertility. Reproductive Biology 16:1-7.

Chen JY, Yang YJ, Meng XY, *et al*., 2024. Oxysophoridine inhibits oxidative stress and inflammation in hepatic fibrosis via regulating Nrf2 and NF-κB pathways. Phytomedicine 132:155585.

Chen Q, Yang W, Wang X, *et al*., 2017. TGF-β1 induces EMT in bovine mammary epithelial cells through the TGF-β1/Smad signaling pathway. Cellular Physiology and Biochemistry 43:82-93.

Cui L, Wang H, Lin J, *et al*., 2020. Progesterone inhibits inflammatory response in E. coli- or LPS-stimulated bovine endometrial epithelial cells by NF-κB and MAPK pathways. Developmental and Comparative Immunology 105:103568.

Dai O, Fan Y, Zhou Q, *et al*., 2025. Effect of Leonurus japonicus alkaloids on endometrial inflammation and its mechanisms. Journal of Ethnopharmacology 342:119432.

Deng L, Zou J, Su Y, *et al*., 2022. Resveratrol inhibits TGF-β1-induced EMT in gastric cancer cells through Hippo-YAP signaling pathway. Clinical and Translational Oncology 24:2210-2221.

Ding H, Wang Y, Li Z, *et al*., 2022. Baogong decoction treats endometritis in mice by regulating uterine microbiota structure and metabolites. Microbial Biotechnology 15:2786-2799.

Haimerl P and Heuwieser W, 2014. Invited review: antibiotic treatment of metritis in dairy cows: a systematic approach. Journal of Dairy Science 97:6649-6661.

Jiang K, Cai J, Jiang Q, *et al*., 2024. Interferon-tau protects bovine endometrial epithelial cells against inflammatory injury by regulating the PI3K/AKT/β-catenin/FoxO1 signaling axis. Journal of Dairy Science 107:555-572.

Katsuno Y and Derynck R, 2021. Epithelial plasticity, epithelial-mesenchymal transition, and the TGF-β family. Developmental Cell 56:726-746.

Korotkov SM, 2023. Mitochondrial oxidative stress is the general reason for apoptosis induced by different-valence heavy metals in cells and mitochondria. International Journal of Molecular Sciences 24:14459.

Lamouille S, Xu J and Derynck R, 2014. Molecular mechanisms of epithelial-mesenchymal transition. Nature Reviews Molecular Cell Biology 15:178-196.

LeBlanc SJ, 2023. Review: postpartum reproductive disease and fertility in dairy cows. Animal 17:100781.

Li X, Wei S, Niu S, *et al*., 2022. Network pharmacology prediction and molecular docking-based strategy to explore the potential mechanism of Huanglian Jiedu Decoction against sepsis. Computers in Biology and Medicine 144:105389.

Loyi T, Kumar H, Nandi S, *et al*., 2015. Expression of pathogen recognition receptors and pro-inflammatory cytokine transcripts in clinical and sub-clinical endometritis cows. Animal Biotechnology 26:194-200.

Mao N, Yu Y, Lu X, *et al*., 2024. Preventive effects of matrine on LPS-induced inflammation in RAW 264.7 cells and intestinal damage in mice through the TLR4/NF-κB/MAPK pathway. International Immunopharmacology 143:113432.

Matsunaga N, Tsuchimori N, Matsumoto T, *et al*., 2011. TAK-242 (resatorvid), a small-molecule inhibitor of Toll-like receptor (TLR) 4 signaling, binds selectively to TLR4 and interferes with interactions between TLR4 and its adaptor molecules. Molecular Pharmacology 79:34-41.

Moustakli E, Stavros S, Katopodis P, *et al*., 2025. Oxidative stress and the NLRP3 inflammasome: focus on female fertility and reproductive health. Cells 14:36.

Osawa T. 2021. Predisposing factors, diagnostic and therapeutic aspects of persistent endometritis in postpartum cows. Journal of Reproduction and Development 67:291-299.

Owens CE, Daniels KM, Ealy AD, *et al*., 2020. Graduate student literature review: potential mechanisms of interaction between bacteria and the reproductive tract of dairy cattle. Journal of Dairy Science 103:10951-10960.

Ru J, Li P, Wang J, *et al*., 2014. TCMSP: a database of systems pharmacology for drug discovery from herbal medicines. Journal of Cheminformatics 6:13.

Ruane PT, Garner T, Parsons L, *et al*., 2022. Trophectoderm differentiation to invasive syncytiotrophoblast is promoted by endometrial epithelial cells during human embryo implantation. Human Reproduction 37:777-792.

Shaukat A, Hanif S, Shaukat I, *et al*., 2024. Up-regulation of inflammatory, oxidative stress, and apoptotic mediators via inflammatory, oxidative stress, and apoptosis-associated pathways in bovine endometritis. Microbial Pathogenesis 191:106660.

Shaukat A, Rajput SA, Hanif S, *et al*., 2025. Morin inhibits inflammation, oxidative stress and ferroptosis in lipopolysaccharide induced endometritis. Pakistan Veterinary Journal 45:799-806.

Sherman BT, Hao M, Qiu J, *et al*., 2022. DAVID: a web server for functional enrichment analysis and functional annotation of gene lists (2021 update). Nucleic Acids Research 50:W216-W221.

Sinha K, Das J, Pal PB, *et al*., 2013. Oxidative stress: the mitochondria-dependent and mitochondria-independent pathways of apoptosis. Archives of Toxicology 87:1157-1180.

Song P, Liu C, Sun M, *et al*., 2022. Oxidative stress induces bovine endometrial epithelial cell damage through mitochondria-dependent pathways. Animals 12:2444.

Sun M, Song P, Zhao Y, *et al*., 2024. Mechanisms of LPS-induced epithelial mesenchymal transition in bEECs. Theriogenology 216:30-41.

Sun Y, Zhou QM, Lu YY, *et al*., 2019. Resveratrol inhibits the migration and metastasis of MDA-MB-231 human breast cancer by reversing TGF-β1-induced epithelial-mesenchymal transition. Molecules 24:1131.

Tang TH, Chang CT, Wang HJ, *et al*., 2013. Oxidative stress disruption of receptor-mediated calcium signaling mechanisms. Journal of Biomedical Science 20:48.

Tian S, Liu T, Jiang J, *et al*., 2024. Salvia miltiorrhiza ameliorates endometritis in dairy cows by relieving inflammation, energy deficiency and blood stasis. Frontiers in Pharmacology 15:1349139.

Wan FC, Zhang C, Jin Q, *et al*., 2020. Protective effects of astaxanthin on lipopolysaccharide-induced inflammation in bovine endometrial epithelial cells. Biology of Reproduction 102:339-347.

Wu H, Dai A, Chen X, *et al*., 2018. Leonurine ameliorates the inflammatory responses in lipopolysaccharide-induced endometritis. International Immunopharmacology 61:156-161.

Xue BX, He RS, Lai JX, *et al*., 2023. Phytochemistry, data mining, pharmacology, toxicology and the analytical methods of Cyperus rotundus L. (Cyperaceae): a comprehensive review. Phytochemistry Reviews 1-46. doi:10.1007/s11101-023-09870-3.

Yao Y, Chen R, Wang G, *et al*., 2019. Exosomes derived from mesenchymal stem cells reverse EMT via TGF-β1/Smad pathway and promote repair of damaged endometrium. Stem Cell Research and Therapy 10:225.

Yu Y, Mao N, Yu L, *et al*., 2025. YiMu-QingGong san alleviates lipopolysaccharide-induced endometritis in mice via inhibiting inflammation and oxidative stress through regulating macrophage polarization. Journal of Ethnopharmacology 337:118992.

Zaatout N, 2022. An overview on mastitis-associated Escherichia coli: pathogenicity, host immunity and the use of alternative therapies. Microbiological Research 256:126960.

Zhang H, Wu ZM, Yang YP, *et al*., 2019. Catalpol ameliorates LPS-induced endometritis by inhibiting inflammation and TLR4/NF-κB signaling. Journal of Zhejiang University Science B 20:816-827.

Zhang W, Li Q and Yin R, 2024. Targeting WEE1 kinase in gynecological malignancies. Drug Design, Development and Therapy 18:2449-2460.

Zhang W and Wu F, 2024. Linoleic acid induces human ovarian granulosa cell inflammation and apoptosis through the ER-FOXO1-ROS-NFκB pathway. Scientific Reports 14:6392.

Zhao M, Wang Y, Li L, *et al*., 2021. Mitochondrial ROS promote mitochondrial dysfunction and inflammation in ischemic acute kidney injury by disrupting TFAM-mediated mtDNA maintenance. Theranostics 11:1845-1863.